A wave roughness Reynolds number parameterization of the sea spray source flux

Sarah J. Norris,[1] Ian M. Brooks,[1] and Dominic J. Salisbury[1]

Received 25 June 2013; accepted 25 July 2013; published 20 August 2013.

[1] Parameterizations of the sea spray aerosol source flux are derived as functions of wave roughness Reynolds numbers, R_{Ha} and R_{Hw}, for particles with radii between 0.176 and 6.61 μm at 80% relative humidity. These source functions account for up to twice the variance in the observations than does wind speed alone. This is the first such direct demonstration of the impact of wave state on the variability of sea spray aerosol production. Global European Centre for Medium-Range Weather Forecasts operational mode fields are used to drive the parameterizations. The source flux from the R_H parameterizations varies from approximately 0.1 to 3 (R_{Ha}) and 5 (R_{Hw}) times that from a wind speed parameterization, derived from the same measurements, where the wave state is substantially underdeveloped or overdeveloped, respectively, compared to the equilibrium wave state at the local wind speed. **Citation:** Norris, S. J., I. M. Brooks, and D. J. Salisbury (2013), A wave roughness Reynolds number parameterization of the sea spray source flux, *Geophys. Res. Lett.*, *40*, 4415–4419, doi:10.1002/grl.50795.

1. Introduction

[2] Sea spray aerosol (SSA) is a dominant contribution to the global atmospheric aerosol loading [*Hoppel et al*., 2002; *Andreae and Rosenfeld*, 2008]; it makes a significant contribution to the scattering of solar radiation, having a cooling influence on the Earth's surface (the aerosol direct effect [*Intergovernmental Panel on Climate Change*, 2007]) of up to 6 W m^{-2} [*Lewis and Schwartz*, 2004]. Highly hygroscopic, SSAs act as efficient cloud condensation nuclei [*Andreae and Rosenfeld*, 2008] and play an important role in determining the microphysical properties of marine clouds. As a sink for aerosol precursor gases, they act as a control on boundary layer nucleation processes [*Merikanto et al*., 2009]. Understanding the magnitude and variability of SSA production is essential to constraining estimates of preindustrial aerosol forcing of climate and estimating future climate, to accurately interpreting satellite data, and as a forcing term for global chemistry transport models and aerosol models.

[3] SSA is produced at the ocean surface by the bursting of bubbles generated primarily by breaking waves (radii of roughly 0.01–10 μm and 1–300 μm from film and jet drops, respectively) and the tearing of water droplets from wave crests (R > 200 μm) [*Lewis and Schwartz*, 2004]. Most parameterizations of SSA production (sea spray source functions) are specified either as simple functions of the mean wind speed [e.g., *Smith et al*., 1993; *Hoppel et al*., 2002] or as a production flux per unit area of whitecap scaled by the total surface whitecap fraction [e.g., *Monahan et al*., 1986; *Mårtensson et al*., 2003], which is in turn usually parameterized as a function of wind speed, most commonly using *Monahan and O'Muircheartaigh* [1980].

[4] In spite of decades of study, there remains an uncertainty of at least an order of magnitude in sea spray source functions [*de Leeuw et al*., 2011]. Wind speed alone cannot explain the observed variability in either SSA flux [*de Leeuw et al*., 2011] or whitecap fraction [*Anguelova and Webster*, 2006]. Water temperature and salinity [*Mårtensson et al*., 2003; *Zabori et al*., 2012] affect bubble properties via the viscosity and surface tension of water and the salt concentration in the droplets forming SSA. A larger source of variability is believed to result from the wave state [*de Leeuw et al*., 2011]; however, few studies of the SSA flux have made coincident, detailed measurements of wave properties.

[5] A joint measure of wind and wave state may be defined as a Reynolds number. Various formulations have been used to characterize wave breaking [*Toba and Koga*, 1986], whitecap fraction [*Zhao and Toba*, 2001; *Goddijn-Murphy et al*., 2011], and sea spray production [*Zhao et al*., 2006; *Shi et al*., 2009; *Liu et al*., 2012], although these last are all theoretical and do not provide evidence of a sea state dependence of the SSA flux. Here we use a wave Reynolds number R_H introduced by *Zhao and Toba* [2001]:

$$R_H = \frac{u_* H_s}{v}, \tag{1}$$

where u_* is the friction velocity, H_s is the significant wave height, and v is a kinematic viscosity. Two variants were proposed: R_{Ha} defined using the viscosity of air, v_a, and R_{Hw} using the viscosity of water v_w. The latter was considered conceptually more robust for processes related to wave breaking and has since been used by *Woolf* [2005] and *Goddijn-Murphy et al*. [2011].

2. Measurements

[6] We use the direct eddy covariance SSA flux data set of *Norris et al*. [2012] and calculate the Reynolds numbers, R_{Ha} and R_{Hw}. All data were collected during cruise D317 of the RRS *Discovery* in the northeast Atlantic, from 21 March to 12 April 2007, as part of the Sea Spray, Gas Flux, and Whitecap (SEASAW) project, a UK contribution to the international Surface Ocean-Lower Atmosphere Study program [*Brooks et al*., 2009a]. Eddy covariance estimates of the

Additional supporting information may be found in the online version of this article.

[1]Institute of Climate and Atmospheric Science, School of Earth and Environment, University of Leeds, Leeds, UK.

Corresponding author: S. J. Norris, Institute of Climate and Atmospheric Science, School of Earth and Environment, University of Leeds, Woodhouse Lane, Leeds LS2 9JT, UK. (snorris@env.leeds.ac.uk)

0094-8276/13/10.1002/grl.50795

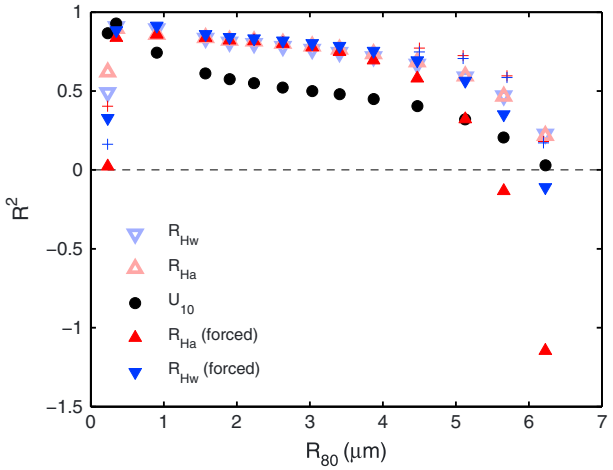

Figure 1. The R^2 values for the fits of the observed source flux to U_{10} (black), both R_{Ha} (red triangle) and R_{Hw} (blue inverted triangle) with fits forced through $R_{Ha}=7100$ and $R_{Hw}=7.2\times10^4$, and unconstrained (pink and pale blue). For those channels affected by poor counting statistics in the two lowest Reynolds number bins, R^2 is also shown after removing those points (plus sign).

SSA flux were made with a collocated sonic anemometer and Compact Lightweight Aerosol Spectrometer Probe (CLASP) [*Hill et al.*, 2008]. The Reynolds numbers were calculated from in situ measurements. H_s was determined from measurements of the one-dimensional wave spectra by a MKIV shipborne wave recorder [*Tucker and Pitt*, 2001], while u_* was measured via direct eddy covariance. ν_a and ν_w are calculated from measurements of air temperature and pressure using the Sutherland equation [*Montgomery*, 1947] and of water temperature and salinity [*Sharqawy et al.*, 2010], respectively. Details of all instrumentation are given in *Brooks et al.* [2009b]. The turbulent flux calculations are described in *Norris et al.* [2012] and *Sproson et al.* [2013]. *Norris et al.* [2012] also discuss the mean meteorological and oceanographic conditions.

3. Results

[7] Sea spray source fluxes for individual CLASP size channels, adjusted to 80% relative humidity, are bin averaged by R_{Ha} and R_{Hw} and linear fits determined (see supporting information). Poor statistics in the two lowest R_H bins results in unconstrained fits predicting a physically unrealistic positive SSA flux at $R_H=0$ for both the smallest and largest particles. *Toba and Koga* [1986] found a threshold of $R_B=1000$ for the onset of wave breaking, where $R_B=u_*^2/\nu_a\omega_p$ is the breaking wave Reynolds number and ω_p is the peak angular frequency of the wind waves. Fitting measured R_H to R_B values, we find critical values of $R_{Ha}=7100\pm2800$ and $R_{Hw}=(7.2\pm2.9)\times10^4$; both agree closely with the intercepts of R_{Ha} and R_{Hw} at zero flux obtained from unconstrained fits across the middle of the measured size range (see supporting information). Below these threshold values, we do not expect wave breaking to occur, and thus, the SSA flux should be zero; we thus force linear fits of the flux to R_H through zero at these thresholds. The gradient, α, and intercept, β, of the linear fits are parameterized as functions of R_{80}—the particle radius at 80% humidity—to define a SSA source function in terms of the Reynolds numbers:

$$\frac{dF}{dR_{80}}=\alpha R_H+\beta. \tag{2}$$

[8] For R_{Ha}, we find

$$\log_{10}(\alpha)=-1.802\times10^{-3}R_{80}^4+0.0215R_{80}^3-0.0236R_{80}^2 -0.9386R_{80}+0.844 \tag{3}$$
$$\beta=-44030e^{-1.91R_{80}},$$

and for R_{Hw}

$$\log_{10}(\alpha)=-1.56\times10^{-3}R_{80}^4+0.0179R_{80}^3-5.8\times10^{-3}R_{80}^2 -0.969R_{80}-0.139 \tag{4}$$
$$\beta=-46380e^{-1.96R_{80}}.$$

[9] No assumptions were made about the functional forms; these were chosen purely on the grounds of the best fit to the data. The R^2 values for the fits against both R_{Ha} and R_{Hw} are shown in Figure 1 along with those for the fits against the 10 m wind speed, U_{10}, from *Norris et al.* [2012]. The Reynolds numbers explain much more of the observed variability in the source flux than does U_{10} alone over most of the measured size range—by 20–60% between 1 and 4 μm, and almost a factor of 2 for R_{Hw} at 5 μm; however, R^2

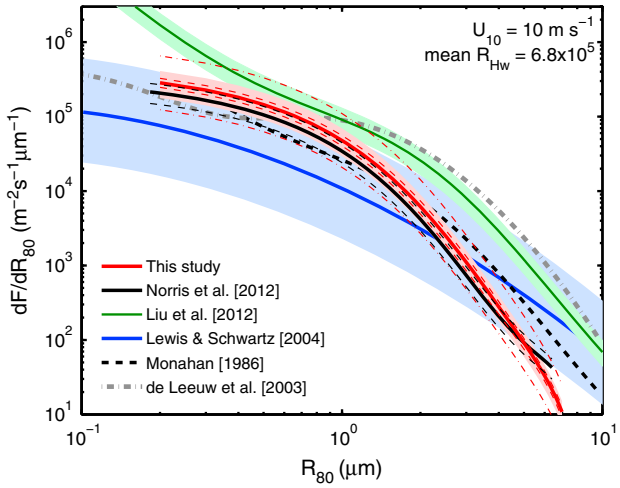

Figure 2. The R_{Hw}-dependent source function from (4) compared with a number of recent functions at $U_{10}=10\,m\,s^{-1}$. Parameterization (4) is plotted for the mean observed value of R_{Hw} for $9.5<U_{10}<10.5\,m\,s^{-1}$. Three different sources of uncertainty are shown: the pick shaded region indicates the range of fluxes resulting from the range of observed R_{Hw} ($4.5\times10^5<R_{Hw}<9.5\times10^5$); the red dashed lines indicate the 95% confidence intervals in the best fit to α and β, and the red dash-dotted line indicates the uncertainty associated with the 95% confidence intervals on the fits of the raw flux estimates to R_{Hw}. The pale green area indicates the uncertainty in *Liu et al.* [2012] resulting from the observed range of R_B values within the wind speed range. The pale blue area is the published uncertainty in the *Lewis and Schwartz* [2004] parameterization. Thin black dashed lines indicate the uncertainty in the *Norris et al.* [2012] function.

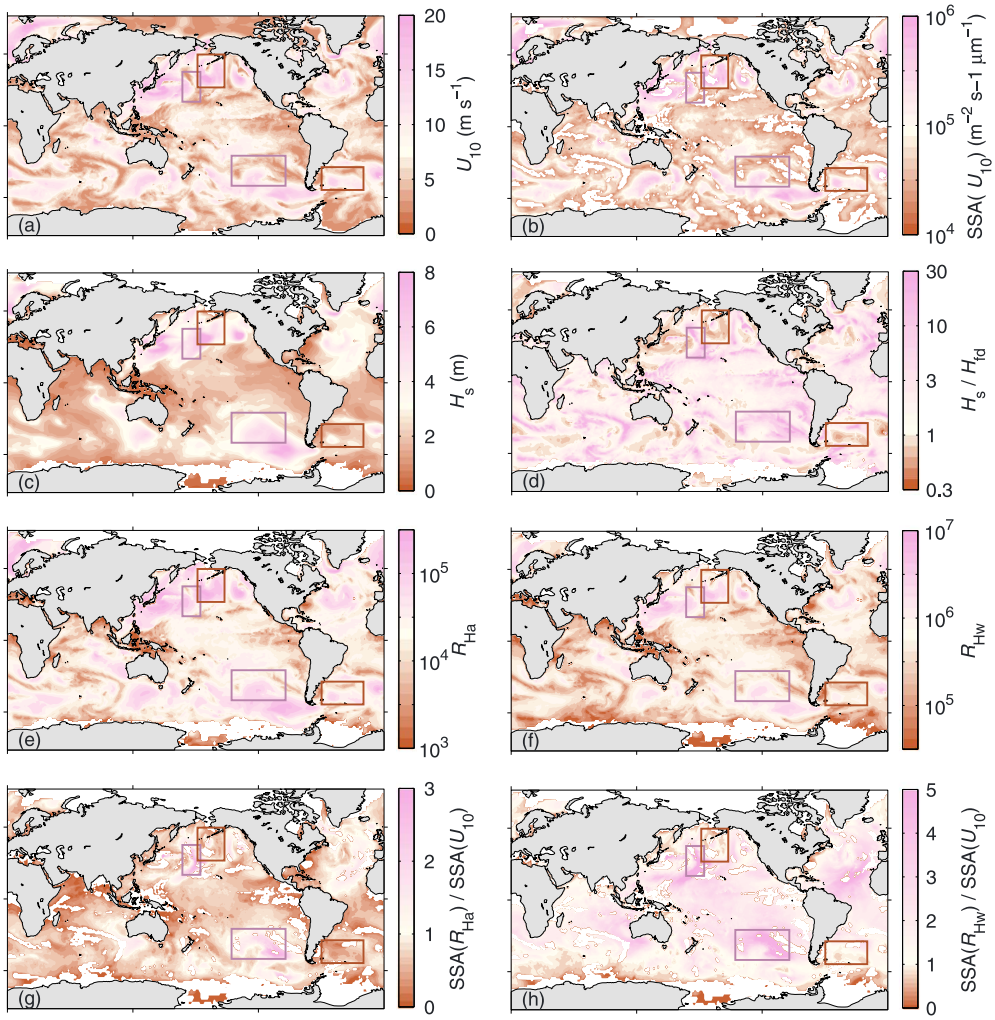

Figure 3. Global distributions of (a) wind speed, U_{10}; (b) SSA flux from *Norris et al*. [2012]; (c) significant wave height, H_s; (d) H_s/H_{fd}; (e) R_{Ha}; (f) R_{Hw}; (g) ratio of sea spray source flux dF/dR_{80} from the R_{Ha} (3) and U_{10} [*Norris et al*., 2012] parameterizations at $R_{80} = 0.5$ µm; and (h) same as Figure 3g but for R_{Hw}. Example regions where the Reynolds number function is significantly higher/lower than the U_{10} function are indicated by purple/brown boxes.

decreases substantially for the smallest and largest size channels where the small number of data points available results in a large uncertainty. R_{Hw} does slightly better than R_{Ha}, increasingly so as particle size increases. Their formulations differ only in the viscosity used; these have very narrow ranges ($1.36–1.42 \times 10^{-5}$ m^2 s^{-1} for ν_a, $1.32–1.45 \times 10^{-6}$ m^2 s^{-1} for ν_w) compared to those of u_* (0.11–0.80 m s^{-1}) and H_s (1.91–5.08 m) within the SEASAW data set. This results from narrow temperature ranges for air (4.7–12.0°C) and water (8.8–12.1°C) (see supporting information). If the points with poor counting statistics are excluded from the analysis, the R^2 values increase substantially (Figure 1), though they still drop off rapidly for $R_{80} > 5$ µm.

[10] The new parameterization (4) is compared with several existing functions in Figure 2 (the alternative parameterization (3) (not shown) gives near-identical results). Because most of these functions depend on wind speed only, we evaluate (4) at the mean R_{Hw} observed over the specified wind speed range during SEASAW and show an uncertainty range corresponding to the range of R_{Hw}. We include the source function of *Liu et al*. [2012] formulated in terms of R_B to combine the whitecap function of *Zhao and Toba* [2001] and sea spray source function of *Monahan* [1986]. Again, this function is evaluated for mean and limiting values of R_B within the wind speed bin.

[11] In order to evaluate the potential impact of accounting for wave state on the SSA source flux, we calculate the flux from both the U_{10}-dependent function of *Norris et al*. [2012] and (3) and (4) using the European Centre for Medium-Range Weather Forecasts (ECMWF) operational mode global fields for 0000 UTC 1 January 2011. U_{10} and H_s are taken directly from the model, while u_* is calculated from U_{10} and the wave model's sea state-dependent drag coefficient [*Janssen*, 2000]. Salinity is taken from the 2009 World Ocean Atlas [*Antonov et al*., 2010]. The ratio between the source fluxes from (3) and (4) and *Norris et al*. [2012] is shown in Figure 3 for $R_{80} = 0.5$ µm. Also shown are fields of U_{10}, the *Norris et al*. [2012] source flux, R_{Ha}, R_{Hw}, H_s, and the ratio H_s/H_{fd} where H_{fd} is the value of H_s for waves in equilibrium with the local wind, calculated from the WAM model wind-wave relation [*Wave Model Development and Implementation Group*, 1988]; H_s/H_{fd} gives a measure of the degree of wave development. In order to avoid any bias that might result from extrapolating the source functions

beyond the range of conditions from which they were derived, we have excluded grid points with winds outside the observed range of $4 < U_{10} < 18\ m\ s^{-1}$.

[12] There are some substantial differences between the parameterizations; the R_{Ha} parameterization ranges from less than 0.1 of the U_{10} source function to about 3 times larger; the R_{Hw} function peaks at 5 times larger. A comparison of the spatial distribution of the differences to those of the forcing parameters is revealing. Consider first the R_{Ha} function (Figure 3g). The regions where its ratio with the U_{10} function is largest coincide not with the highest winds or Reynolds numbers in storm systems, but around the margins of these systems. These are regions where the wavefield is significantly better developed than the equilibrium wavefield for the local wind ($H_s/H_{fd} > 1$); two such regions are indicated by purple boxes. In regions where the wave state is underdeveloped compared to the equilibrium state—notably in the regions of highest wind speed within storm systems—the R_{Ha} parameterization falls below the U_{10} parameterization; examples are indicated by the brown boxes. The R_{Hw} parameterization follows a similar spatial pattern but predicts somewhat higher fluxes over the tropical and subtropical oceans. This is a consequence of the stronger temperature dependence of water viscosity compared to that of air. The implications of this and the limitations it imposes on the interpretation of our results are discussed below.

4. Conclusions

[13] New parameterizations of the sea spray source flux ($0.176 < R_{80} < 6.61\ \mu m$) have been derived as functions of wave Reynolds numbers, R_{Ha} and R_{Hw}. They account for up to twice the variance in the measured fluxes than does wind speed alone. The variance explained decreases with particle size for all three parameterizations; at the smallest sizes, U_{10} and R_H account for similar variance, and that explained by U_{10} then falls more rapidly with particle size than that for R_{Ha} and R_{Hw}. The size dependence of R^2 is consistent with *Norris et al*. [2013] who found that SSA production per unit area whitecap was wind speed dependent for $R_{80} < 2\ \mu m$, but showed no clear relationship at larger sizes. We speculate that this behavior is related to changes in bubble populations with increasing wind and wave breaking—*Norris et al*. [2013] found that concentrations of small bubbles increased more than those of large bubbles with increasing wind speed—and the sizes of aerosol particles generated by different-sized bubbles. Here, jet drops will dominate production for $R_{80} > 1\ \mu m$ and film drops for $R_{80} < 1\ \mu m$.

[14] A comparison of the ratio of the new parameterizations to the wind speed-dependent function derived by *Norris et al*. [2012] from the same data set shows differences of a factor of 0.1 to 3 (R_{Ha}) and 5 (R_{Hw}). Fluxes higher than those of the U_{10} function are found around the margins of storm systems where propagation of waves away from the regions of highest winds results in wave states that are overdeveloped compared to the equilibrium state for the local wind. Fluxes lower than those from the U_{10} function are found where the wave state is underdeveloped. We emphasize that both the U_{10} and R_H-dependent source functions are derived from the same in situ measurements; differences between them arise almost entirely from the inclusion of information on wave state via the Reynolds number. Superficially, the results appear contrary to those of *Norris et al*. [2012] that the flux was higher in undeveloped seas for a given wind speed. In fact, there is no direct contradiction. *Norris et al*. [2012] characterized wave development by the mean wave slope; this depends only on H_s and T_z, the zero-crossing period of the waves, and says nothing about the relationship between the observed waves and those expected under equilibrium with the local wind.

[15] The R_{Hw} function predicts larger fluxes than R_{Ha} over much of the ocean—a result of the stronger temperature dependence of viscosity for water than for air. The observations used to derive the source functions span a limited range of temperatures. This leaves open the possibility that viscosity-dependent properties of wave breaking or bubbles might affect the SSA flux in a manner not accounted for by these source functions. Measurements under a much wider range of conditions are required to address this issue. The data set is also not large enough to assess any separate impact of wind waves and swell, nor of relative wind and wave directions, both of which may complicate the wind-wave-flux relationship [e.g., *Goddijn-Murphy et al*., 2011]. Thus, the source functions proposed cannot be considered universal but are a significant step toward this goal and an improvement on simple wind speed-dependent functions.

[16] At any given time, the wave state over the majority of the world's oceans is out of equilibrium with the local wind—the majority being overdeveloped and dominated by swell; just 8.5% is found to be underdeveloped in the ECMWF fields by the Wave Model Development and Implementation definition. Simple wind speed-dependent SSA source functions will tend to misrepresent the spatial variability of SSA production. This has implications for modeling of new particle formation and regional aerosol budgets, marine atmospheric boundary layer chemistry, and the spatial variability of cloud condensation nuclei concentrations over the oceans. The new parameterizations are readily implemented in models and should lead to better representation of the spatial and temporal variability of sea spray fluxes.

[17] **Acknowledgments.** This work was funded by the UK Natural Environment Research Council grants NE/C001842/1 as part of UK SOLAS, NE/G00353X/1, and NE/G000107/1. We thank the Captain and crew of the RRS *Discovery* and the staff of National Marine Facilities Sea Systems for their assistance in preparing for and during the cruise, ECMWF for the global model reanalysis fields, and David Woolf and an anonymous reviewer for their constructive comments on the manuscript.

[18] The Editor thanks David Woolf and an anonymous reviewer for their assistance in evaluating this paper.

References

Andreae, M. O., and D. Rosenfeld (2008), Aerosol-cloud-precipitation interactions, Part 1. The nature and sources of cloud-active aerosols, *Earth-Sci. Rev.*, *89*, 13–41, doi:10.1016/j.earscirev.2008.03.001.

Anguelova, M. D., and F. Webster (2006), Whitecap coverage from satellite measurements: A first step toward modeling the variability of oceanic whitecaps, *J. Geophys. Res.*, *111*, C03017, doi:10.1029/2005JC003158.

Antonov, J. I., D. Seidov, T. P. Boyer, R. A. Locarnini, A. V. Mishonov, H. E. Garcia, O. K. Baranova, M. M. Zweng, and D. R. Johnson (2010), in *World Ocean Atlas 2009, Volume 2: Salinity*, edited by S. Levitus, 184 pp., NOAA Atlas NESDIS 69, U.S. Government Printing Office, Washington, D.C.

Brooks, I. M., et al. (2009a), Physical exchanges at the air-sea interface: Field measurements from UK-SOLAS, *Bull. Am. Meteorol. Soc.*, *90*, 629–644, doi:10.1175/2008BAMS2578.1.

Brooks, I. M., et al. (2009b), UK-SOLAS field measurements of air-sea exchange: Instrumentation, *Bull. Am. Meteorol. Soc.*, *90*, (electronic supplement), 9–16, doi:10.1175/2008BAMS2578.2.

de Leeuw, G., E. L. Andreas, M. D. Anguelova, C. W. Fairall, E. R. Lewis, C. O'Dowd, M. Schulz, and S. E. Schwartz (2011), Production flux of sea-spray aerosol, *Rev. Geophys.*, *49*, RG2001, doi:10.1029/2010RG000349.

Goddijn-Murphy, L., D. K. Woolf, and A. H. Callaghan (2011), Parameterizations and algorithms for oceanic whitecap coverage, *J. Phys. Oceanogr.*, *41*, 742–756, doi:10.1175/2010JPO4533.1.

Hill, M. K., B. J. Brooks, S. J. Norris, M. H. Smith, I. M. Brooks, G. de Leeuw, and J. J. N. Lingard (2008), A Compact Lightweight Aerosol Spectrometer Probe (CLASP), *J. Atmos. Oceanic Technol.*, *25*, 1996–2006, doi:10.1175/2008JTECHA1051.1.

Hoppel, W. A., G. M. Frick, and J. W. Fitzgerald (2002), The surface source function for sea-salt aerosol and aerosol dry deposition to the ocean surface, *J. Geophys. Res.*, *107*(D19), 4382, doi:10.1029/2001JD002014.

Intergovernmental Panel on Climate Change (2007), *Climate Change 2007: The Physical Science Basis: Working Group I Contribution to the Fourth Assessment Report of the Intergovernmental Panel on Climate Change*, edited by S. Solomon et al., 996 pp., Cambridge Univ. Press, New York.

Janssen, P. A. E. M. (2000), ECMWF wave modeling and satellite altimeter wave data, in *Satellites, Oceanography and Society*, edited by D. Halpern, pp. 35–56, Elsevier, Amsterdam.

Lewis, E. R., and S. E. Schwartz (2004), *Sea Salt Aerosol Production: Mechanisms, Methods, Measurements, and Models—A Critical Review*, Geophys. Monogr. Ser., vol. *152*, 413 pp., AGU, Washington, D. C.

Liu, B., C. L. Guan, L. A. Xie, and D. L. Zhao (2012), An investigation of the effects of wave state and sea spray on an idealized typhoon using an air–sea coupled modelling system, *Adv. Atmos. Sci.*, *29*, 391–406, doi:10.1007/s00376-011-1059-7.

Mårtensson, E. M., E. D. Nilsson, G. de Leeuw, L. H. Cohen, and H. C. Hansson (2003), Laboratory simulations and parameterization of the primary marine aerosol production, *J. Geophys. Res.*, *108*(D9), 4297, doi:10.1029/2002JD002263.

Merikanto, J., D. V. Spracklen, G. W. Mann, S. J. Pickering, and K. S. Carslaw (2009), Impact of nucleation on global CCN, *Atmos. Chem. Phys.*, *9*, 8601–8616, doi:10.5194/acp-9-8601-2009.

Monahan, E. C. (1986), The ocean as a source for atmospheric particles, in *The Role of Air-Sea Exchange in Geochemical Cycling*, Buat-Menard, edited by D. Reidel, 129–163 pp., Publishing Company, Dordrecht.

Monahan, E., and I. O'Muircheartaigh (1980), Optimal power-law description of oceanic whitecap coverage dependence on wind speed, *J. Phys. Oceanogr.*, *10*, 2094–2099.

Monahan, E. C., D. E. Spiel, and K. L. Davidson (1986), A model of marine aerosol generation via whitecaps and wave disruption, in *Oceanic Whitecaps*, edited by E. C. Monahan and G. Mac Niocaill, pp. 167–174, D. Reidel Publishing Company, Dordrecht.

Montgomery, R. B. (1947), Viscosity and thermal conductivity of air and diffusivity of water vapor in air, *J. Meteorol.*, *4*, 193–196.

Norris, S. J., I. M. Brooks, M. K. Hill, B. J. Brooks, M. H. Smith, and D. A. J. Sproson (2012), Eddy covariance measurements of the sea spray aerosol flux over the open ocean, *J. Geophys. Res.*, *117*, D07210, doi:10.1029/2011JD016549.

Norris, S. J., I. M. Brooks, B. I. Moat, M. J. Yelland, G. de Leeuw, R. W. Pascal, and B. J. Brooks (2013), Field measurements of aerosol production from whitecaps in the open ocean, *Ocean Sci.*, *9*, 133–145, doi:10.5194/os-9-133-2013.

Sharqawy, M. H., J. H. Lienhard, and S. M. Zubair (2010), Thermophysical properties of seawater: A review of existing correlations and data, *Desalin. Water Treat.*, *16*, 354–380, doi:10.5004/dwt.2010.1079.

Shi, J., D. Zhao, X. Li, and Z. Zhong (2009), New wave-dependent formulae for sea spray flux at air-sea interface, *J. Hydrodyn.*, *21*, 573–581.

Smith, M. H., P. M. Park, and I. E. Consterdine (1993), Marine aerosol concentrations and estimated fluxes over the ocean, *Q. J. R. Meteorol. Soc.*, *119*, 809–824, doi:10.1002/qj.49711951211.

Sproson, D. A. J., I. M. Brooks, and S. J. Norris (2013), The effect of hygroscopicity on sea spray aerosol fluxes: A comparison of high-rate and bulk correction methods, *Atmos. Meas. Tech.*, *6*, 323–335, doi:10.5194/amt-6-323-2013.

Toba, Y., and M. Koga (1986), A parameter describing overall conditions of wave breaking, whitecapping, sea-spray production and wind stress, in *Oceanic Whitecaps*, edited by E. C. Monahan and G. Mac Niocaill, pp. 37–47, Springer, New York.

Tucker, M. J., and E. G. Pitt (2001), *Waves in Ocean Engineering*, Ocean Eng. Book Ser., vol. *5*, 521 pp., Elsevier, New York.

Wave Model Development and Implementation Group (1988), The WAM model: A third generation ocean wave prediction model, *J. Phys. Oceanogr.*, *18*, 1775–1810.

Woolf, D. K. (2005), Parametrization of gas transfer velocities and sea-state-dependent wave breaking, *Tellus*, *57A*, 87–94.

Zábori, J., R. Krejci, A. M. L. Ekman, E. M. Mårtensson, J. Ström, G. de Leeuw, and E. D. Nilsson (2012), Wintertime Arctic Ocean sea water properties and primary marine aerosol concentrations, *Atmos. Chem. Chem. Phys.*, *12*, 0405–10421, doi:10.5194/acp-12-10405-2012.

Zhao, D., and Y. Toba (2001), Dependence of whitecap coverage on wind and wind-wave properties, *J. Oceanogr.*, *57*, 603–616.

Zhao, D., Y. Toba, K. Sugioka, and S. Komori (2006), New sea spray generation function for spume droplets, *J. Geophys. Res.*, *111*, C02007, doi:10.1029/2005JC002960.